Neurosci. Bull. February, 2016, 32(1):99–107
DOI 10.1007/s12264-015-0003-8

www.neurosci.cn
www.springer.com/12264

REPORT

TNP-ATP is Beneficial for Treatment of Neonatal Hypoxia-Induced Hypomyelination and Cognitive Decline

Jie Xiao[1] · Yilong Huang[1] · Xia Li[1] · Longjun Li[1] · Ting Yang[1] · Lixuan Huang[1] · Ling Yang[1] · Hong Jiang[1] · Hongchun Li[1] · Fan Li[1]

Received: 13 August 2015 / Accepted: 17 November 2015 / Published online: 15 January 2016

Abstract Our previous study together with other investigations have reported that neonatal hypoxia or ischemia induces long-term cognitive impairment, at least in part through brain inflammation and hypomyelination. However, the detailed mechanisms are not fully understood. Here, we used a rodent model of neonatal hypoxia by subjecting postnatal day 0 (P0) rat pups to systemic hypoxia (3.5 h). We found that neonatal hypoxia increased the glutamate content and initiated inflammatory responses at 4 h and 1 day after hypoxia, caused hypomyelination in the corpus callosum, and impaired hippocampus-dependent learning and memory when assessed 30–60 days after hypoxia. Interestingly, much of the hypoxia-induced brain damage was ameliorated by treatment with the ATP analogue 2′,3′-0-(2,4,6-trinitrophenyl)-adenosine 5′-triphosphate (TNP-ATP; blocks all ionotropic P2X1-7 receptors), whereas treatment with pyridoxalphosphate-6-azophenyl-2′,4′-disulphonic acid (PPADS; inhibits P2X1-3 and P2X5-7 receptors) was less neuroprotective. Our data indicated that activation of ionotropic ATP receptors might be partially, if not fully, involved in glutamate deregulation, neuroinflammation, hypomyelination, and cognitive dysfunction after neonatal hypoxia.

Keywords Neonatal hypoxia · Inflammation · Ionotropic ATP receptors · Glutamate · Memory deficit

Introduction

Hypoxic ischemic encephalopathy (HIE) is an important cause of mortality in the neonatal period and is associated with high morbidity [1]. It is mainly characterized by neurological deficits such as cognitive dysfunction, which is believed to be the consequence of hypoxia-induced brain damage, in which the impairment of white matter myelination and inflammatory responses have been commonly observed in the HIE model [2–6]. While the underlying mechanism remains elusive, the white matter abnormalities in the periventricular zone due to oligodendrocyte precursor cell (OPC) and oligodendrocyte (OL) damage are associated with hypomyelination and cognitive dysfunction after hypoxia or ischemia [7–10]. Given that glutamate is increased after HIE [11] and that glutamate excitotoxicity plays a crucial role in the cell death of OLs and OPCs after hypoxia in immature brain [12, 13], hypoxia- or ischemia-induced glutamate malfunction may be one of the causative factors for white matter myelination deficits due to OL and OPC cell loss.

The glutamate increase and accumulation in extracellular space after hypoxia has been associated with neuroinflammation, in which inflammatory cytokines impair the functions of glutamate transporters such as glutamate transporter 1 (GLT-1, also known as excitatory amino acid transporter 2 (EAAT2)), glutamate-aspartate transporter (GLAST, also known as EAAT1), excitatory amino-acid carrier 1 (EAAC1), and EAAT4 [14–17], resulting in inhibition of glutamate clearance after hypoxia. Therefore, suppressing hypoxia-induced neuroinflammation might modulate the glutamate deregulation and its associated hypomyelination/dysfunction in the brain.

It is also known that hypoxia triggers a sustained increase of extracellular ATP, which acts as a danger signal in the

Jie Xiao and Yilong Huang have contributed equally to this work.

✉ Fan Li
leefan623@sina.com

[1] Department of Pathology and Pathophysiology, School of Basic Medical Science, Kunming Medical University, Kunming 650500, China

brain and may cause microglial activation, neuroinflammatory responses, and neuronal damage. Such actions have been discussed in a recent review summarizing P2X7, P2Y1, and A2A receptors [18]. In a previous study, we found that ionotropic P2X4 ATP receptors, predominantly expressed in amoeboid microglial cells at the early developmental stage, are significantly upregulated by neonatal hypoxia [19]. Furthermore, in an *in vitro* culture system, inactivation of P2X4 receptors attenuates the hypoxia-induced expression and release of inflammatory cytokines such as IL-1β. However, until recently, few studies have investigated the role of P2X4 ATP receptors as a potentially useful therapeutic option for the treatment of hypoxia-induced brain injury in neonates. Given that a number of studies have demonstrated elevated microglial activation and IL-1β expression and release in the brain after hypoxia at the neonatal stage [3, 20], and this inflammatory response is closely associated with hypomyelination and cognitive deficits in HIE models [4, 21], we hypothesized that activation of ATP receptors (possibly multiple subtypes, particularly of the P2X4 ATP receptor) in the brain after neonatal hypoxia contributes to neuroinflammation, glutamate deregulation, hypomyelination, and long-term cognitive deficits. However, this investigation was limited by the lack of selective subtype-specific inhibitors with good aqueous solubility.

There is growing evidence that 5-(3-bromophenyl)-1,3-dihydro-2H-benzofuro [3,2-e]-1,4-diazepin-2-one (5-BDBD) works as a selective P2X4 receptor antagonist [22–26]. However, 5-BDBD has poor solubility in saline, which limits its application in neonates using systemic injection. Although both ATP analogues 2′,3′-0-(2,4,6-trinitrophenyl)-adenosine 5′-triphosphate (TNP-ATP) and pyridoxalphosphate-6-azophenyl-2′,4′-disulphonic acid (PPADS) have effects on multiple targets, TNP-ATP blocks all P2X1–7 ionotropic receptors while PPADS inhibits P2X1–3 and P2X5–7 ATP receptors. This discrepancy has been used to assay the potential role of P2X4 receptors [27, 28]. Therefore, in the present study, using a systemic hypoxia model we described previously [19], we addressed whether TNP-ATP or PPADS administration *in vivo* is beneficial in the treatment of systemic hypoxia-induced brain injury in neonates, as well as the possible role of P2X4 receptors.

Materials and Methods

Animals

The animal care and experimental protocol was approved by the Animal Care and Use Committee of Kunming Medical University in accordance with the International Guiding Principles for Animal Research as stipulated by the Council for International Organizations of Medical Sciences (1985). Sprague-Dawley rats and their offspring were group-housed, with *ad libitum* access to water and food, under a 12-h light/dark cycle and a thermoregulated environment. Postnatal day 0 (P0) rat pups (either sex) were used for modeling systemic hypoxia. All efforts were made to minimize the number of rats used and their suffering. The rats were sacrificed by cervical dislocation under deep isoflurane anesthesia. The experimental protocol and animal usage are illustrated in Fig. 1A. The persons who performed the behavioral tests and brain imaging were blind to the treatment and group information.

Systemic Hypoxia and Drug Administration

Systemic hypoxia was induced as described previously [19]. Briefly, P0 rat pups were kept in a hypoxia chamber (Chinese Utility Model Patent; patent No. ZL 2013 2 010770. 6) filled with nitrogen and 5% oxygen and maintained at 28 ± 0.5 °C for 3.5 h or as otherwise stated. Then the rats were allowed to recover under normoxic conditions for the indicated time (hypoxia group; Hy). Meanwhile, some littermates were kept outside of the chamber as normoxic matching controls (normal control group; NG). A single dose of PPADS dissolved in saline (5, 10, 20, or 40 mg/kg; Sigma-Aldrich, St. Louis, MO) or TNP-ATP dissolved in saline (1, 2, 4, or 8 mg/kg; Sigma-Aldrich) was injected intraperitoneally (i.p.) into Hy or NG rats 2 h after the hypoxia exposure. Saline was injected as the vehicle control.

Glutamate Measurement

Glutamate content in the entire periventricular area was measured using ultrahigh performance liquid chromatography (UPLC; Waters, Milford, MA) tandem mass spectrometry (MS) equipped with an API3200 detector (AB, Los Angeles, CA). Four hours or 1 day after systemic hypoxia exposure, the periventricular zone of the brain was dissected (male and female, $n = 4$–6 per group), homogenized, and sonicated with formic acid, followed by centrifugation at 12,000 rpm for 20 min. The supernatant was collected and filtered with a 0.2-μm membrane filter. The filtered supernatant (5 μL) was separated on an Acquity UPLC BEH C18 column (internal diameter 2.1 mm, length 100 mm, 1.7 μm particle size) maintained at 30 °C. The mixed mobile phase delivered at 0.3 mL/min was water–acetonitrile (40:60, *v*/*v*), containing 0.1% formic acid. The MS system was operated in the positive ion mode for glutamate detection. Multiple reaction monitoring at unit resolution was used to monitor the transitions of the molecular ions of glutamate at m/z 148.0–84.1 or at m/z 148.0–130.1. Other optimized MS parameters were: curtain

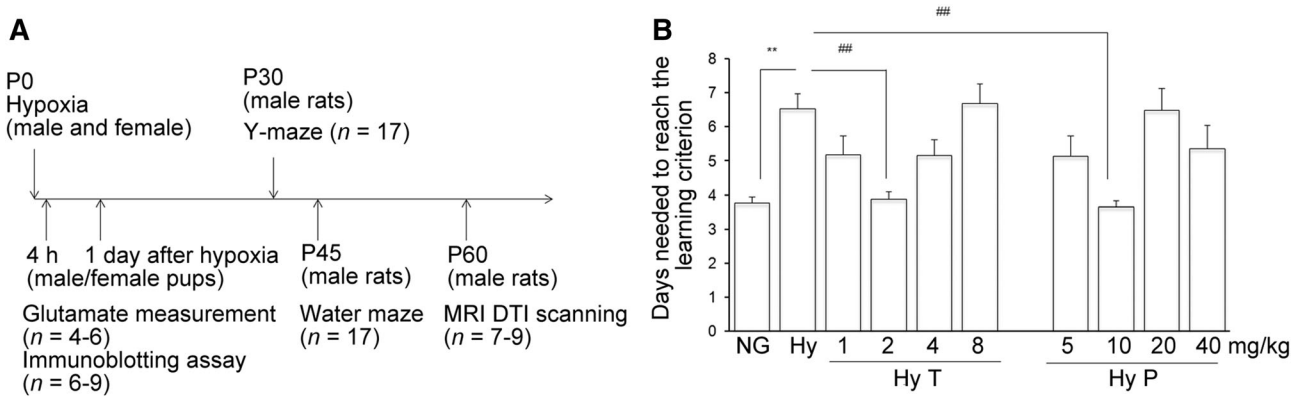

Fig. 1 Learning and memory in a Y-maze task after hypoxia with/without PPADS/TNP-ATP treatment. **A** Schematic of the experimental protocol and animal usage. **B** In P30 rats, the average number of days needed to reach the learning criterion was obtained from a Y-maze test ($n = 17$ animals/group; $^{**}P < 0.01$ *vs* NG; $^{\#\#}P < 0.01$ *vs* Hy, mean ± SEM, Kruskal-Wallis test with Mann-Whitney U *post-hoc* test). NG, normal control group; Hy, systemic hypoxia-exposed (3.5 h) group; Hy P, hypoxic mice treated with PPADS 2 h after hypoxia; Hy T, hypoxic mice treated with TNP-ATP 2 h after hypoxia.

gas, gas 1, and gas 2 were at 15, 60, and 65 psi, respectively; ion spray voltage, 5500 V; ion source temperature, 650 °C; de-clustering potential, 13 V. The dwell time was 200 ms. Data were collected and analyzed using the system-equipped software.

Immunoblotting Assay

The cerebral tissues containing the periventricular area and hippocampi were collected 4 h or 1 day after hypoxia ($n = 6$–9 male and female rats per group), lysed, and proteins were extracted using a kit (Biovision, Milpitas, CA) containing proteinase inhibitors, DTT, and phosphatase inhibitors (Roche, Penzberg, Germany) following the manufacturer's protocol. The supernatant was collected after centrifugation at 12,000 rpm for 10 min, and total protein concentration was determined using a Bradford kit (Beyotime, NanJing, China). Equal amounts of protein (20 μg) were loaded and separated on 10% sodium dodecyl sulfate-polyacrylamide gel (Beyotime), and then transferred to polyvinylidene difluoride membrane (Millipore, Billerica, MA) at 4 mA/cm^2 for 70 min in a mixture of Tris-glycine buffer (TBS) and 20% (*v*/*v*) methanol. The membrane was blocked in TBS-Tween 20 0.2% (TBST) buffer containing 5% non-fat dry milk for 1 h at room temperature, and then incubated and gently shaken overnight (at 4 °C) with primary antibody in TBST containing 5% non-fat dry milk, followed by incubation with the corresponding secondary antibody for 1 h at room temperature. The primary antibodies were mouse anti-Iba1/ALF1 monoclonal IgG (1:1500, Wako Chemicals, Richmond, VA), rabbit anti-IL-1β polyclonal IgG (1:2000, Abcam, Cambridge, UK), rabbit anti-EAAT1 (1:300, Santa Cruz, CA), mouse anti-EAAT2 (1:800, Abcam), and mouse anti-β-actin (1:20000, Abcam). The secondary antibodies were horseradish peroxidase conjugated anti-rabbit monoclonal IgG (1:3000, Abmart, Shanghai, China) and anti-mouse monoclonal IgG (1:2000–20000, Abmart). Proteins were visualized using a chemiluminescence substrate system (Millipore, Billerica, MA) on a chemiluminescence imaging system (Bio-Rad Laboratories, Hercules, CA). Page Ruler pre-stained protein ladders (Thermo Fisher Scientific, Waltham, MA) were used as the molecular weight markers. Band optical density was quantified using Image J (National Institutes of Health, Bethesda, MD; http://rsb.info.nih.gov/ij/, 1997–2006) and normalized to β-actin intensity.

Y-maze Test

Y-maze tests were performed to evaluate learning and memory as described previously [29, 30]. Briefly, male rats ($n = 17$ per group) at postnatal day 30 (P30) were trained to learn and remember the illumination signal for escaping an electric shock with 20 trials per day as reported previously [29]. The escape latency into the safe arm was recorded. The trial was considered successful if the latency was <10 s. When a rat showed 90% successful trials in a day, it was considered to have reached the learning criterion. The number of days that animals took to reach the criterion was recorded.

Morris Water Maze Test

After completion of the Y-maze test, the same animals (P45 male, $n = 17$ per group) were subjected to the Morris water maze test [31] to evaluate spatial reference learning and memory. Following an initial 2-min swimming session,

the rats were trained to locate the hidden platform during four trials per day for another 5 days. One day after the last training session, each animal was given a 120-s probe test, in which the submerged platform was removed and the animal was expected to enter the target quadrant and make more entries into the location that previously contained the platform (memory retention). Time spent in the target quadrant and the number of crosses of the platform location in the probe test were recorded using a video tracking system.

7-T MRI DTI Scanning

A group of rats (P60 male, $n = 7$–9 per group) were randomly selected after completion of the Morris water maze test and subjected to MRI scanning [32]. All MRI measurements were acquired using a 7-T Bruker scanner with a maximum gradient of 360 mT/m (Bruker BioSpec 70/20USR (Ettlingen, Germany). A 200-mm birdcage transmit-only RF coil for transmitting and an actively decoupled receive-only quadrature surface coil were used for adult brain MRI. Whole-brain diffusion T2-weighted images were acquired with the following parameters: repetition time (TR), 3000.0 ms; echo time (TE), 36.0 ms; resolution, 256 × 256; FA (flip angle): 180.0°, SI: 0.80/0.80 mm, FOV (field of view): 3.50 cm^2, MTX (matrix): 256, pos (position): 0.40 mm 1:1, TurboRA- RE-T2 3:1. The diffusion T2-C-weighted images were acquired with the following parameters: TR, 2000.0 ms; TE, 36.0 ms; FA, 180.0°; SI, 0.80/0.80 mm; FOV, 3.50 cm^2; MTX, 256; pos, 2.00 mm 1:1; TurboRARE-T2-C 4:1. Diffusion tensor images (DTIs) were acquired using an echo planar imaging (EPI) sequence: TR, 6000.0 ms; TE, 26.0 ms; FA, 90.0°; Slice thickness(SI)/Interlayer spacing(IS), 0.80/0.80 mm; FOV, 3.50 cm^2; MTX, 128 (a); EPI-diffusion-tensor 5:1; 24 continuous slices between olfactory bulb and medulla oblongata were scanned. DTIs were analyzed using Superconduction Magnet System software (JANIS Research Company, MA) and the fractional anisotropy (FA) maps of the corpus callosum (CC) and middle corpus callosum (MCC) from sections 9/24 to 22/24 were each averaged to generate a mean FA image.

Statistical Analysis

All data are presented as mean ± SEM. The Mann-Whitney U test, Kruskal-Wallis test, and Friedman test were used to determine the statistical significance of data that are not normally distributed. Statistical analyses were performed with SPSS (IBM, Chicago, IL). $P < 0.05$ was considered to be statistically significant.

Results and Discussion

TNP-ATP Ameliorates Cognitive Dysfunction after Systemic Hypoxia

Consistent with our previous finding [19], systemic hypoxia in P0 rat pups induced long-term cognitive deficits when tested at P30 (Fig. 1B). Animals exposed to hypoxia required significantly more days of training to reach the learning criterion in the Y-maze than control rats (Fig. 1B). Interestingly, blockade of ionotropic ATP receptors by PPADS or TNP-ATP (injected 2 h after hypoxia) dose-dependently reduced the number of days to criterion, with a peak effect at 10 mg/kg for PPADS (Fig. 1B, $P < 0.01$) and 2 mg/kg for TNP-ATP (Fig. 1B, $P < 0.01$), while treatment with PPADS or TNP-ATP did not affect the number of days to criterion in control rats (data not shown). These results suggest that activation of ionotropic ATP receptors might be associated with cognitive deficits after neonatal hypoxia, at least as measured by the Y-maze task 30 days after hypoxia.

It should be noted that ionotropic ATP receptors, especially the P2X3 and P2X4 subtypes, play a critical role in pain perception [27, 33–37]. Therefore, the performance in the pain-based Y-maze task may be masked by changes in pain perception after hypoxia or drug administration. To confirm the possible roles of TNP-ATP or PPADS in cognition, we further validated the role of TNP-ATP in hypoxia-induced cognitive impairment, using the Morris water maze test that assesses spatial learning and memory without pain-related shock stimulation. Compared to the normal control group, animals subjected to neonatal hypoxia showed a significantly longer escape latency to find the hidden platform on days 3–5 (Fig. 2A). In the probe test after 5 days of training, both the time spent in the target quadrant (Fig. 2B) and the number of crossings of the platform region (Fig. 2C) were significantly lower in rats exposed to hypoxia than the control group. Administration of TNP-ATP (2 mg/kg) significantly increased the time spent in the target quadrant (Fig. 2B) and the number of crossings of the platform region (Fig. 2C) in hypoxia-exposed animals. However, PPADS (10 mg/kg) failed to increase the time spent in the target quadrant (Fig. 2B) but partially restored the platform crossings (Fig. 2C). Neither TNP-ATP nor PPADS had significant effects on the Morris water maze performance of normal controls (data not shown). Our data suggested that TNP-ATP administration ameliorates systemic hypoxia-induced cognitive dysfunction in the Morris water maze task as well.

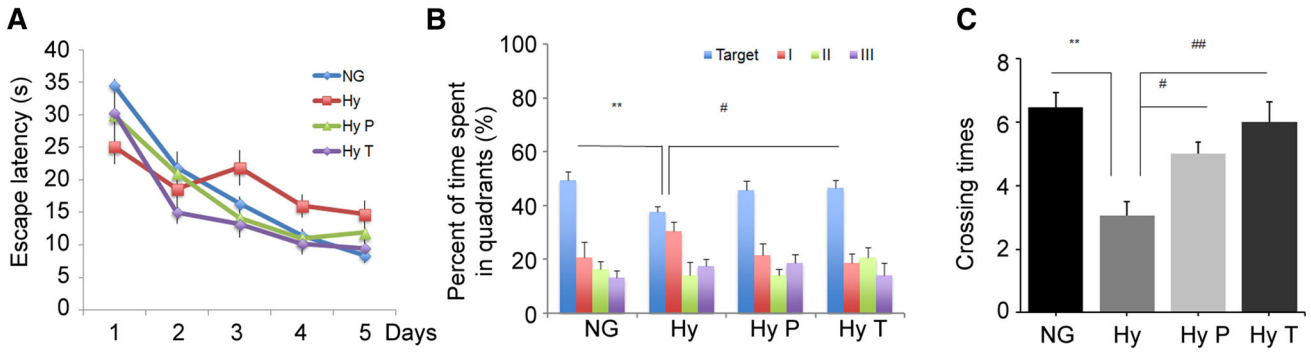

Fig. 2 Learning and memory alterations in the Morris water maze task after hypoxia with/without PPADS/TNP-ATP treatment. **A** Escape latencies of indicated groups during training sessions. **B**, **C** Time spent in the quadrants (**B**) and the number of crossings of the platform region (**C**) in the probe test of the Morris water maze test. NG, normal control group; Hy, systemic hypoxia-exposed (3.5 h) group; Hy P, hypoxic mice treated with PPADS (10 mg/kg) 2 h after hypoxia; Hy T, hypoxic mice treated with TNP-ATP (2 mg/kg) 2 h after hypoxia. $n = 17$ animals per group. $^{**}P < 0.01$ *vs* NG group; $^{\#}P < 0.05$; $^{\#\#}P < 0.01$ *vs* Hy group. Mean ± SEM, Kruskal–Wallis test with Mann–Whitney U *post-hoc* test.

TNP-ATP Administration Is Neuroprotective Against Neonatal Hypoxia-Induced Hypomyelination

Since it is known that hypomyelination commonly occurs in the HIE model, and is believed to be associated with cognitive deficits [2–6], here we tested whether systemic hypoxia has long-term effects on the development of white matter myelination, and investigated the role of TNP-ATP in white matter injury after neonatal hypoxia. Compared to the normal brain, MRI T2 images showed expanded septum and lateral ventricles in the hypoxic brain (Fig. 3A, B), and T2-C images revealed destroyed myelin structure in the CC region (Fig. 3E, F). These deleterious effects of hypoxia were attenuated by TNP-ATP (Fig. 3D, H), but PPADS had no evident protective effects (Fig. 3C, G). At P60, significantly lower FA values were found in the CC (Fig. 3M) and MCC (Fig. 3N) in the hypoxic group than in controls (Fig. 3I, J, O, P), demonstrating that long-term persistent hypomyelination/white matter impairment occurred after systemic hypoxia in neonates. In addition, administration of TNP-ATP rather than PPADS restored the FA values in both the CC (Fig. 3K–P) and MCC regions (Fig. 3K–P). Our data suggested that TNP-ATP administration protects the white matter against hypoxia in neonates.

TNP-ATP Administration Suppresses Inflammation and Glutamate Increase After Systemic Neonatal Hypoxia

Since our previous study showed that TNP-ATP treatment attenuates the hypoxia-induced expression and release of the inflammatory cytokine IL-1β *in vitro* [19], we next investigated whether TNP-ATP suppresses the inflammatory response in the brain, which could be one of the mechanisms for offering neuroprotection after systemic hypoxia. We found that IL-1β was significantly increased from 4 h to 1 day after hypoxia (Fig. 4A). Although treatment with TNP-ATP for a short time period did not prevent this elevated IL-1β level, it significantly reduced the level when measured on day 1 after hypoxia (Fig. 4A). Administration of PPADS only showed a slight decrease of IL-1β on day 1 after hypoxia, but failed to reach statistical significance (Fig. 4A). Neither TNP-ATP nor PPADS changed the IL-1β expression and release in control rats (data not shown).

It is known that glutamate-mediated neurotoxicity is the major trigger for neuronal damage after hypoxia, and glutamate malfunctions are associated with neuroinflammation and white matter impairment. Furthermore, inflammatory cytokines impair the functions of glutamate transporters such as EAAT1 and EAAT2 [14–17] leading to the inhibition of glutamate clearance after hypoxia. So, we then evaluated the effect of TNP-ATP on hypoxia-induced glutamate deregulation. Similar to the finding that neonatal hypoxia increases the glutamate content in brain [11, 38], we found that systemic hypoxia exposure significantly increased the total glutamate in the periventricular zone, even at 4 h after hypoxia (Fig. 4B). The glutamate levels remained high in the hypoxia group until 1 day after exposure (Fig. 4B). TNP-ATP treatment significantly prevented the glutamate elevation at 4 h and on day 1 (Fig. 4B) while PPADS only showed protection at 4 h after hypoxia (Fig. 4B). Surprisingly, we detected upregulation of EAAT1 (Fig. 4C) and EAAT2 (Fig. 4D) from 4 h to 1 day after hypoxia, which were not affected by TNP-ATP. But PPADS decreased the EAAT2 upregulation on day 1 after hypoxia. These results suggested that elevation of glutamate content by hypoxia is prevented by TNP-ATP although the clearance processes seem not to be modulated.

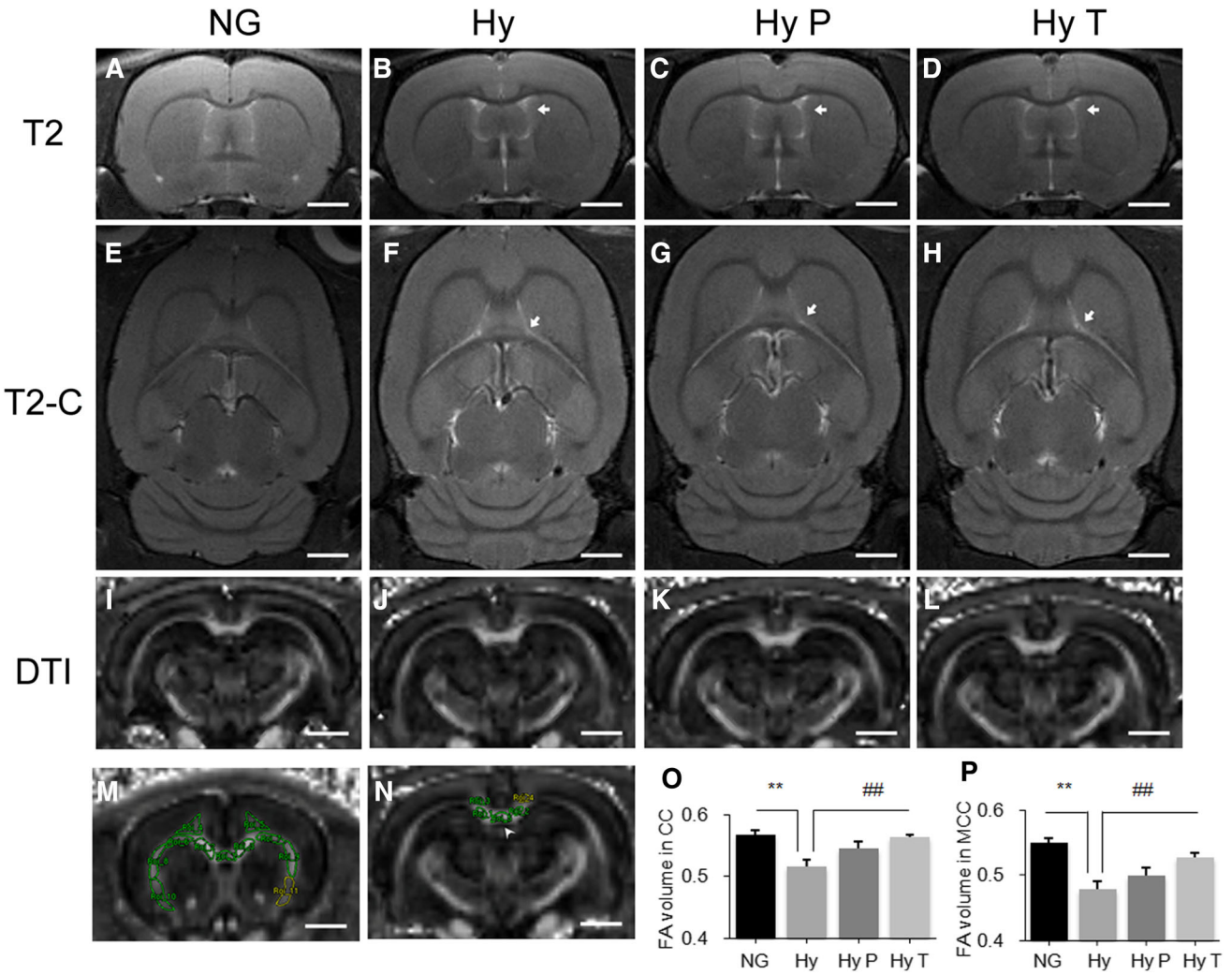

Fig. 3 7-T MRI/DTI images and FA values in targeted regions of interest (ROI). **A–L**, Representative T2, T2-C, and DTI images from scanning section 13 (with a clear CCM structure) of P60 rats from the indicated groups. *Arrows* in T2 images indicate expanded septum and lateral ventricles. *Arrows* in T2-C images indicate regions with reduced myelin sheaf direction and destroyed myelin structure. **M**, **N** Images of the corpus callosum (CC) (**M**) and mid-CC (MCC) (**N**) areas where the FA values were calculated. *Scale bars*, 2.5 mm. **O**, **P** Averaged FA values of CC (**O**) and MCC (**P**). $n = 7$–9 animals per group. Hy, hypoxia group; Hy P, hypoxic mice treated with PPADS (10 mg/kg); Hy T, hypoxic mice treated with TNP-ATP (2 mg/kg); NG, normal control group. $^{**}P < 0.01$ *vs* NG group. $^{\#\#}P < 0.01$ *vs* Hy group. Mean ± SEM, Kruskal–Wallis test with Mann–Whitney U *post-hoc* test.

Since a previous study indicated that microglial activation triggered by neonatal hypoxia increases the glutamate content in brain [38], we propose that this mechanism might be at least one of the reasons for the increased glutamate concentration in neonates exposed to hypoxia in this study. Blockade of ATP receptors by TNP-ATP or PPADS would suppress microglial activation, which might consequently attenuate the regulation of glutamate induced by hypoxia in the immature rodent brain.

In the early development stages, microglial cells are mainly located in the periventricular area [19] with high expression of P2X4 receptors, although other types are not excluded. This might be the reason why TNP-ATP is more effective in attenuating the periventricular white matter damage and cognitive deficit induced by neonatal hypoxia. In a previous study, the combination of TNP-ATP and PPADS was used to indicate the possible role of P2X4 receptors [27], thus, our results might also suggest that the activation of one or more specific subtypes of ATP receptor (including P2X4) is involved in systemic hypoxia-induced cognitive impairment. However, this requires further study using either more selective inhibitors of the P2X4 receptor or genetic manipulations to confirm or deny the role of P2X4 in hypoxia-induced brain impairments in neonates. Indeed, there is increasing evidence suggesting that 5-BDBD works as a selective P2X4 receptor antagonist [22–26]; thus, successful treatment of hypoxic animals with 5-BDBD would provide confirmative evidence for a role of

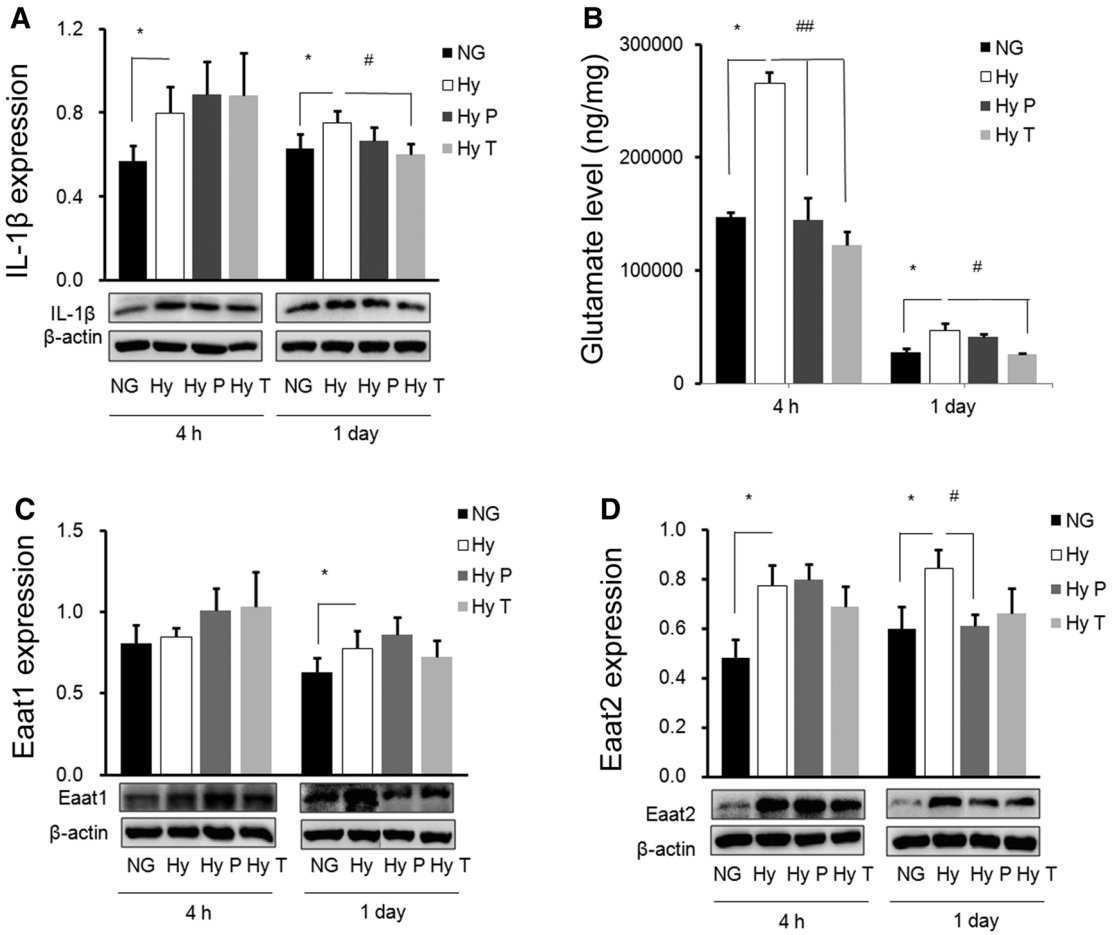

Fig. 4 Expression levels of IL-1β, glutamate content, EAAT1, and EAAT2 after hypoxia. **A** Representative Western blots and quantification of IL-1β in the indicated groups. Band intensity was calculated using arbitrary units (AU) and normalized to β-actin. $n = 6$–9 animals per group. **B** Glutamate content measured by UPLC-MS at indicated time points. $n = 4$–6 animals per group. **C**, **D** Representative Western blots and quantification of EAAT1 (**C**) and EAAT2 (**D**) at indicated times. $n = 6$–9 animals per group. Hy, hypoxia group; Hy P, hypoxic mice treated with PPADS (10 mg/kg); Hy T, hypoxic mice treated with TNP-ATP (2 mg/kg); NG, normal control group. $^{*}P < 0.05$ *vs* NG group. $^{\#}P < 0.05$, $^{\#\#}P < 0.01$ *vs* Hy group. Mean ± SEM, non-parametric Friedman test.

P2X4 in neuroprotection. However, 5-BDBD has poor solubility in saline and must be dissolved in DMSO, which limits its application by systemic injection, especially in neonatal pups. An alternative strategy to confirm the protective role of P2X4 ATP receptors against hypoxia-induced brain damage would be to use P2X4-null animals. At present, no P2X4 knock-out rats are available and we were unable to access P2X4-null mice. Therefore, further investigations are needed to identify the possible role of P2X4 in HIE.

Our results from TNP-ATP and PPADS treatment could not exclude the possible effects of P2X7 and P2Y1 receptors on brain injury due to systemic neonatal hypoxia [39]. In addition, it has been reported that A2A adenosine receptors are involved in hypoxia-induced damage [40, 41]. Both TNP-ATP and PPADS inhibit ecto-nucleotidases, which may generate adenosine after injection [18, 42]. The generated adenosine may interact with A2A receptors and contribute to brain damage after hypoxia. Given that TNP-ATP is more potent than PPADS in the blockade of ecto-nucleotidases [42], the different effects of TNP-ATP and PPADS on hypoxia-impaired learning and memory may come from their effects on adenosine generation and A2A receptor activation.

In summary, systemic hypoxia in neonates induced glutamatergic deregulation, neuroinflammation, hypomyelination, and long-term cognitive deficits. Treatment of neonates with TNP-ATP significantly ameliorated these effects. While other possibilities cannot be excluded, the effect of TNP-ATP on ionotropic ATP receptors might be part of the mechanism. Further investigations are required to dissect the role of specific subtypes of ATP receptors in HIE.

Acknowledgments This work was supported by grants from the National Natural Science Foundation of China (81200939 and 31260242), National Science and Technology Supporting Plan of

China (2014BAI01B00), Natural Science Foundation of Yunnan Province, China (2011FB060), the National Undergraduate Innovation Fund of China (201310678001), and the Undergraduate Innovation Fund of Yunnan Province, China (6011202105). We are grateful to Prof. Shuqing Li at the Department of Pathology and Pathophysiology, School of Basic Medical Science, Kunming Medical University for his support throughout the study.

References

1. de Vries LS, Jongmans MJ. Long-term outcome after neonatal hypoxic-ischaemic encephalopathy. Arch Dis Child Fetal Neonatal Ed 2010, 95: F220–224.
2. Deng Y, Xie D, Fang M, Zhu G, Chen C, Zeng H, *et al.* Astrocyte-derived proinflammatory cytokines induce hypomyelination in the periventricular white matter in the hypoxic neonatal brain. PLoS One 2014, 9: e87420.
3. Kaur. C, Sivakumar. V, Zou. Z, Ling. E-A. Microglia-derived proinflammatory cytokines tumor necrosis factor-alpha and interleukin-1beta induce Purkinje neuronal apoptosis via their receptors in hypoxic neonatal rat brain. Brain Struct Funct 2014, 219: 151–170.
4. Fatemi A, Wilson MA, Phillips AW, McMahon MT, Zhang J, Smith SA, *et al.* In vivo magnetization transfer MRI shows dysmyelination in an ischemic mouse model of periventricular leukomalacia. J Cereb Blood Flow Metab 2011, 31: 2009–2018.
5. Meng S, Qiao M, Scobie K, Tomanek B, Tuor UI. Evolution of magnetic resonance imaging changes associated with cerebral hypoxia-ischemia and a relatively selective white matter injury in neonatal rats. Pediatr Res 2006, 59: 554–559.
6. Wang S, Wu EX, Tam CN, Lau HF, Cheung PT, Khong PL. Characterization of white matter injury in a hypoxic-ischemic neonatal rat model by diffusion tensor MRI. Stroke 2008, 39: 2348–2353.
7. Suryana E, Jones NM. The effects of hypoxic preconditioning on white matter damage following hypoxic-ischaemic injury in the neonatal rat brain. Int J Dev Neurosci 2014, 37: 69–75.
8. Kaur C, Ling EA. Periventricular white matter damage in the hypoxic neonatal brain: role of microglial cells. Prog Neurobiol 2009, 87: 264–280.
9. Cengiz P, Uluc K, Kendigelen P, Akture E, Hutchinson E, Song C, *et al.* Chronic neurological deficits in mice after perinatal hypoxia and ischemia correlate with hemispheric tissue loss and white matter injury detected by MRI. Dev Neurosci 2011, 33: 270–279.
10. Huang Z, Liu J, Cheung PY, Chen C. Long-term cognitive impairment and myelination deficiency in a rat model of perinatal hypoxic-ischemic brain injury. Brain Res 2009, 1301: 100–109.
11. Pu Y, Li QF, Zeng CM, Gao J, Qi J, Luo DX, *et al.* Increased detectability of alpha brain glutamate/glutamine in neonatal hypoxic-ischemic encephalopathy. AJNR Am J Neuroradiol 2000, 21: 203–212.
12. Ikonomidou C, Price MT, Mosinger JL, Frierdich G, Labruyere J, Salles KS, *et al.* Hypobaric-ischemic conditions produce glutamate-like cytopathology in infant rat brain. J Neurosci 1989, 9: 1693–1700.
13. Zonouzi M, Renzi M, Farrant M, Cull-Candy SG. Bidirectional plasticity of calcium-permeable AMPA receptors in oligodendrocyte lineage cells. Nat Neurosci 2011, 14: 1430–1438.
14. Rossi DJ, Brady JD, Mohr C. Astrocyte metabolism and signaling during brain ischemia. Nat Neurosci 2007, 10: 1377–1386.
15. Schousboe A, Waagepetersen HS. Glial modulation of GABAergic and glutamat ergic neurotransmission. Curr Top Med Chem 2006, 6: 929–934.
16. Sheldon AL, Robinson MB. The role of glutamate transporters in neurodegenerative diseases and potential opportunities for intervention. Neurochem Int 2007, 51: 333–355.
17. Yi JH, Hazell AS. Excitotoxic mechanisms and the role of astrocytic glutamate transporters in traumatic brain injury. Neurochem Int 2006, 48: 394–403.
18. Rodrigues RJ TAaCR. ATP as a multi-target danger signal in the brain. Front Neurosci 2015, 9.
19. Li F, Wang L, Li JW, Gong M, He L, Feng R, *et al.* Hypoxia induced amoeboid microglial cell activation in postnatal rat brain is mediated by ATP receptor P2X4. BMC Neurosci 2011, 12: 111.
20. Yan YG, Zhang J, Xu SJ, Luo JH, Qiu S, Wang W. Clustering of surface NMDA receptors is mainly mediated by the C-terminus of GluN2A in cultured rat hippocampal neurons. Neurosci Bull 2014, 30: 655–666.
21. Savard A, Lavoie K, Brochu ME, Grbic D, Lepage M, Gris D, *et al.* Involvement of neuronal IL-1β in acquired brain lesions in a rat model of neonatal encephalopathy. J Neuroinflammation 2013, 10: 110.
22. Balazs B, Danko T, Kovacs G, Koles L, Hediger MA, Zsembery A. Investigation of the inhibitory effects of the benzodiazepine derivative, 5-BDBD on P2X4 purinergic receptors by two complementary methods. Cell Physiol Biochem 2013, 32: 11–24.
23. Barr TP, Hrnjic A, Khodorova A, Sprague JM, Strichartz GR. Sensitization of cutaneous neuronal purinergic receptors contributes to endothelin-1-induced mechanical hypersensitivity. Pain 2014, 155: 1091–1101.
24. Chen K, Zhang J, Zhang W, Zhang J, Yang J, Li K, *et al.* ATP-P2X4 signaling mediates NLRP3 inflammasome activation: a novel pathway of diabetic nephropathy. Int J Biochem Cell Biol 2013, 45: 932–943.
25. Gofman L, Cenna JM, Potula R. P2X4 receptor regulates alcohol-induced responses in microglia. J Neuroimmune Pharmacol 2014, 9: 668–678.
26. Wu T, Dai M, Shi XR, Jiang ZG, Nuttall AL. Functional expression of P2X4 receptor in capillary endothelial cells of the cochlear spiral ligament and its role in regulating the capillary diameter. Am J Physiol Heart Circ Physiol 2011, 301: H69–78.
27. Tsuda M, Shigemoto-Mogami Y, Koizumi S, Mizokoshi A, Kohsaka S, Salter MW, *et al.* P2X4 receptors induced in spinal microglia gate tactile allodynia after nerve injury. Nature 2003, 424: 778–783.
28. Horvath RJ, DeLeo JA. Morphine enhances microglial migration through modulation of P2X4 receptor signaling. J Neurosci 2009, 29: 998–1005.
29. Zou W, Wang HX, Liu J, Zhang H, An LJ. Expression of caveolin-1 protein in the rat brain and its role in the discrimination learning. Acta Physiologica Sin 2006, 58: 429–434.
30. Zhang Y, Qiao L, Song M, Wang L, Xie J, Feng H. HPLC-ESI-MS/MS analysis of the water-soluble extract from Ziziphi spinosae semen and its ameliorating effect of learning and memory performance in mice. Pharmacogn Mag 2014, 10: 509–516.
31. Li ZQ, Li LX, Mo N, Cao YY, Kuerban B, Liang YX, *et al.* Duration-dependent regulation of autophagy by isoflurane exposure in aged rats. Neurosci Bull 2015, 31: 505–513.
32. Fang F, Lei H. Increased hippocampal T2 in a rat model of pentylenetetrazol-induced kindling correlates with seizure scores. J Neurol Sci 2010, 292: 16–23.
33. Burnstock G. Purinergic P2 receptors as targets for novel analgesics. Pharmacol Ther 2006, 110: 433–454.
34. Nakatsuka T, Gu JG. P2X purinoceptors and sensory transmission. Pflugers Arch 2006, 452: 598–607.
35. Tsuda M, Kuboyama K, Inoue T, Nagata K, Tozaki-Saitoh H, Inoue K. Behavioral phenotypes of mice lacking purinergic P2X4 receptors in acute and chronic pain assays. Mol Pain 2009, 5: 28.

36. Gum RJ, Wakefield B, Jarvis MF. P2X receptor antagonists for pain management: examination of binding and physicochemical properties. Purinergic Signal 2012, 8: 41–56.
37. Horvath RJ, Romero-Sandoval EA, De Leo JA. Inhibition of microglial P2X4 receptors attenuates morphine tolerance, Iba1, GFAP and mu opioid receptor protein expression while enhancing perivascular microglial ED2. Pain 2010, 150: 401–413.
38. Sivakumar V, Ling EA, Lu J, Kaur C. Role of glutamate and its receptors and insulin-like growth factors in hypoxia induced periventricular white matter injury. Glia 2010, 58: 507–523.
39. Kylhammar D, Bune LT, Radegran G. P2Y(1) and P2Y(1)(2) receptors in hypoxia- and adenosine diphosphate-induced pulmonary vasoconstriction in vivo in the pig. Eur J Appl Physiol 2014, 114: 1995–2006.
40. Chen JF, Eltzschig HK, Fredholm BB. Adenosine receptors as drug targets–what are the challenges? Nat Rev Drug Discov 2013, 12: 265–286.
41. Fredholm BB, Chen JF, Cunha RA, Svenningsson P, Vaugeois JM. Adenosine and brain function. Int Rev Neurobiol 2005, 63: 191–270.
42. Ziganshin AU, Ziganshina LE, King BF, Pintor J, Burnstock G. Effects of P2-purinoceptor antagonists on degradation of adenine nucleotides by ecto-nucleotidases in folliculated oocytes of Xenopus laevis. Biochem Pharmacol 1996, 51: 897–901.